Journal of Materials Chemistry A

COMMUNICATION

Cite this: *J. Mater. Chem. A*, 2018, **6**, 24092

Received 27th August 2018
Accepted 12th November 2018

DOI: 10.1039/c8ta08324j

rsc.li/materials-a

Direct microencapsulation of pure polyamine by integrating microfluidic emulsion and interfacial polymerization for practical self-healing materials†

He Zhang,[ab] Xin Zhang,[c] Chenlu Bao,[d] Xin Li,[e] Dawei Sun,[fg] Fei Duan,[b] Klaus Friedrich[h] and Jinglei Yang *[f]

Encapsulation of polyamines for the practical application of self-healing epoxy is promising yet challenging due to their high reactivity and good solubility in water and most organic solvents. Herein, we developed an innovative method to directly synthesize microcapsules containing pure polyamine by integrating microfluidic emulsion and interfacial polymerization. Using this integration to make full use of the advantages and avoid the shortcomings of the involved two techniques, the properties of the fabricated microcapsules could be delicately tailored according to the practical demands of self-healing materials. The superiority of the obtained polyamine microcapsules was demonstrated *via* a dual-microcapsule high-performance self-healing system with fully autonomous recoverability, high thermal and long-term stability, relatively fast healing kinetics. The highest healing efficiency of 111 ± 12% in terms of recovered mode I fracture toughness was achieved at room temperature for 48 h without any external intervention. The high performance, environmental stability, and low cost and toxicity introduced by the robust microcapsules promote the potential practical application of this self-healing system.

[a]*The National Engineering Research Center of Novel Equipment for Polymer Processing, The Key Laboratory of Polymer Processing Engineering (SCUT), Ministry of Education, School of Mechanical and Automotive Engineering, South China University of Technology, Guangzhou, 510641, China. E-mail: maeyang@ust.hk*

[b]*School of Mechanical and Aerospace Engineering, Nanyang Technological University, 639798, Singapore*

[c]*School of Civil and Environmental Engineering, Nanyang Technological University, 639798, Singapore*

[d]*School of Materials Science and Engineering, Tianjin Polytechnic University, Tianjin, 300387, China*

[e]*National Laboratory of Solid State Microstructures, Department of Materials Science and Engineering, Nanjing University, Nanjing 210093, China*

[f]*Department of Mechanical and Aerospace Engineering, Hong Kong University of Science and Technology, Kowloon, Hong Kong, China*

[g]*College of Materials Science and Engineering, Beijing University of Technology, Beijing 100124, China*

[h]*Institute for Composite Materials, Technical University of Kaiserslautern, Kaiserslautern, D-67663, Germany*

† Electronic supplementary information (ESI) available. See DOI: 10.1039/c8ta08324j

1. Introduction

Self-healing materials have the ability to repair damage and restore the lost or degraded properties or performances using resources inherently available to a system without external intervention.[1] Since the pioneering work by White *et al.* in 2001,[2] diverse strategies and chemistries have been explored to realize self-healing function in materials and much progress has been made in this area.[3–10] To date, the development of self-healing materials is still ongoing.[11,12] Although previous works mainly focused on extending the limits of self-healing area to verify its feasibility, one trend is to develop fully autonomous practical self-healing systems with low cost and toxicity, high healing performance and material compatibility, good thermal and long-term stability, and fast healing kinetics.[13] Intrinsic self-healing materials by molecular design have great potential for long-term practical application.[14,15] However, to date, this has only been demonstrated in soft and rubbery polymers with certain human intervention to close cracks due to the local requirement for molecular interaction, and thus was only conceived conceptually for primary verification *via* the bottom-up synthesis route. Currently, the faster and more practical way is to integrate extrinsic carriers with healants into commercial polymeric materials since this strategy can be easily incorporated without modification of the host matrix, while delivering a high healing performance for relatively wide cracks.

After screening all the self-healing chemistries and the forms of extrinsic carriers for self-healing purpose,[3,16–23] the self-healing of thermosetting epoxy by encapsulated two-part amine–epoxy chemistry has the greatest practicability since it perfectly matches the above-mentioned requirements.[24] Previous reports have verified the feasibility of this self-healing system.[25–31] However, a bottleneck still exists for its development, that is, albeit epoxy can be encapsulated easily using various approaches, it is exceedingly challenging to encapsulate polyamine hardener using the existing techniques due to its high reactivity and good solubility in water and most organic solvents. While the former leads to chemical incompatibility of

polyamines with many polymer shell-forming chemistries, the latter results in difficulty for polyamines to form a stable emulsion, which is a prerequisite for traditional encapsulation techniques. Consequently, although there have been several efforts,[25–29,32–34] high-quality polyamine microcapsules still cannot be directly synthesized, hindering the further development of this system, including its theoretical verification and practical application.

Besides, when self-healing materials are targeted for application for encapsulation techniques, it is hard to achieve consistency between application and encapsulation for healants with different physicochemical properties. Contradictions always exist, where the physicochemical properties preferred for an application are adverse to those required for the encapsulation process, and *vice versa*. Higher reactivity for the healant is favorable for autonomous and fast healing without external interventions. Nevertheless, it not only challenges the thermal and long-term stability of both the healant and the corresponding carrier, but also leads to difficulty in its encapsulation *via* existing techniques. Specifically, encapsulability and healing kinetics/speed of a healant fundamentally tend to be mutually exclusive to each other. Therefore, many explored microcapsule-based self-healing systems either need significant external interventions to accelerate the healing reaction or are compromised by their limited healing performance at room temperature. A similar paradox occurs for the molecular structure of healants when traditional encapsulation techniques are adopted. This is especially true for polyamines. Polyamines (such as polyetheramines) that can deliver high healing performances are difficult or even unable to be encapsulated,[25,26,29] while those that can be encapsulated with moderate success (such as ethylenediamine-based condensates or derivatives) are not good candidates for self-healing applications.[28,31–35] The high selectivity of traditional encapsulation techniques for the physicochemical properties of healants greatly restricts the easy tailoring of the core composition of microcapsules according to the practical demands of self-healing materials.

Considering the intrinsic limits of existing encapsulation techniques and the wide applications of encapsulated polyamines, including healants for self-healing, pH triggers for self-reporting,[36–38] and latent curing agents,[33,34] it is necessary to explore new approaches for the synthesis of high-quality polyamine microcapsules. Herein, by integrating microfluidic emulsion and interfacial polymerization,[39] we develop a smart strategy to directly fabricate robust microcapsules containing pure polyamine with great potential for practical self-healing applications.

2. Results and discussion

2.1. Mechanism for encapsulation by integrating microfluidic emulsion and interfacial polymerization

The encapsulation system was elaborately designed to make full use of the advantages but avoid the shortcomings of the involved two traditional encapsulation processes. It consists of three successive steps in the device (Fig. 1): (1) generation of individual polyamine micro-droplets in non-equilibrium by microfluidic T-junction, (2) formation of preliminary microcapsules through instant interfacial polymerization between the core polyamine and diisocyanate in reaction solution, and (3) thickening of their shell at elevated temperature. Since the generated non-equilibrium micro-droplets are immediately enwrapped *via* instant interfacial polymerization, this encapsulation process does not require a stable emulsion, which is a prerequisite for successful encapsulation *via* both microfluidic and interfacial polymerization.[31,34] Polyamine droplets with a controllable size can be generated by tuning the relative feeding rates of polyamine to co-flow solvent in Teflon tubing T1 and T2, respectively, using syringe pumps. As schematically shown in the oval enlargement of the T-junction, the thin continuous polyamine stream breaks down into small individual droplets due to the balance between interfacial tension and shear force.[40,41] Once the stream of mixture in T2 flows into the agitated reaction solution consisting of a non-polar solvent, which is miscible with the co-flow solvent, diisocyanate, surfactant, and catalyst, the co-flow solvent mixes with the solvent and the polyamine diffuses across interface and reacts instantly with the diisocyanate (reaction scheme in Fig. S1†) near the interface to form a polyurea membrane to enwrap the polyamine droplet (circle and dashed circle enlargements in Fig. 1a). The preliminary shell is then thickened in the reaction solution at elevated temperature for a certain duration.

Thus ingenious integration tackles the previously mentioned paradoxes between the encapsulability during encapsulation and delivered performance for the application of polyamines when traditional encapsulation techniques are applied. Due to the complete separation of generating micro-droplets and forming the shell into two independent steps, the encapsulation approach is not selective to the targeting cores and a wide variety of liquid polyamines can be encapsulated regardless of their molecular structures, solubility, reactivity, and compositions. In this study, tetraethylenepentamine (TEPA) and its mixtures with a commercial trifunctional primary amine with soft oxypropylene units in its backbone, *i.e.* JEFFAMINE T403, were adopted for encapsulation. TEPA and JEFFAMINE T403 represent two different types of polyamines and their molecular structures are shown in Fig. S2.† The reason why the solubility of polyamine in the solvents is not crucial is that the diffused polyamine can instantly react with diisocyanate at the interface to thicken the shell rather than dissolve in the solvents, which is attributed to the extremely high reactivity of amine with isocyanate and the adopted high concentration of diisocyanate in the reaction solution. Based on this strategy, polyamines with a higher reactivity are preferred for the encapsulation process, which evidently differs from the prior methods and can solve the paradox about the reactivity of healants for encapsulation and practical application.

The fabricated device functioned as designed and expected (Videos S1–S4†). The typical freeze frames (Fig. 1b) from Videos S1–S3† display the three different zones of the T-junction, showing a thin continuous stream in T2 right after the T-junction and breaking down of the stream into individual droplets in T2 before flowing into the reaction solution. Fig. 1c shows the freeze frames with a time interval of 40 ms from

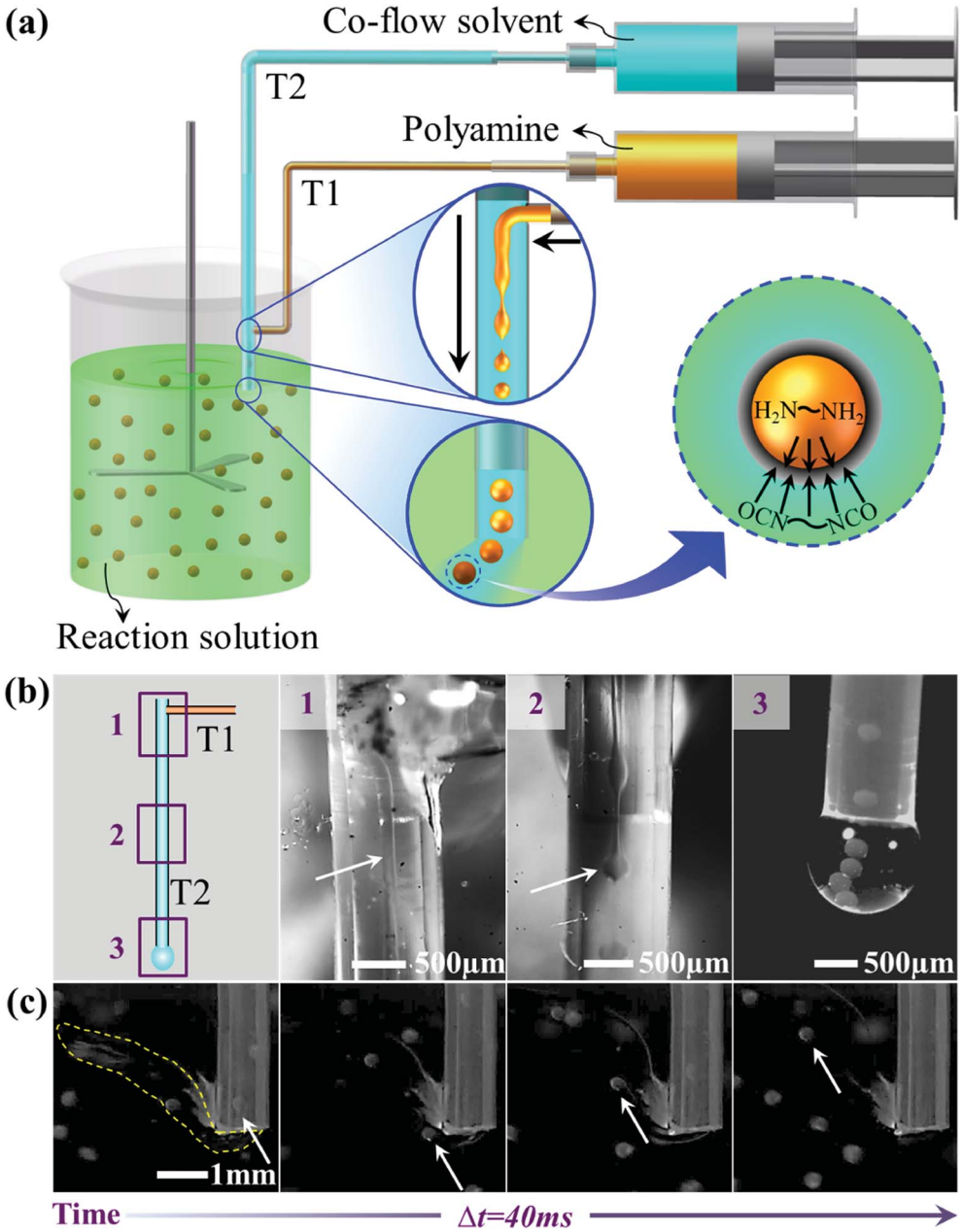

Fig. 1 (a) Mechanism for the encapsulation of pure polyamine by integrating microfluidic T-junction (T1/T2) and interfacial polymerization. (b) Evolution of liquid polyamine from thin continuous stream to individual droplets. The two arrows indicate the thin continuous stream and droplet, respectively. (c) Sequential shell formation around the amine droplet in the flowing reaction solution. Time interval between two neighboring images is 40 ms. The arrows in the figures indicate the evolution of the same TEPA droplet, and the area in dashed curve indicates flowing and mixing of the co-flow solvent with the solvent in the reaction solution. Feeding rates for TEPA and co-flow solvent were 0.02 mL min^{-1} and 0.5 mL min^{-1}, respectively, which were the same for the figures below.

Video S4† for the evolution of a droplet into a microcapsule with the preliminary polyurea membrane upon flowing of the amine droplet into the reaction solution. The area in the dashed curve indicates flowing and mixing of the co-flow solvent with the solvent in the reaction solution. The arrows in the images illustrate the change of a certain droplet from the end of T2 to the reaction solution. In addition, other individual microcapsules can be seen, which were generated early. The preliminary microcapsules generated at this step with feeding rates of 0.02 mL min^{-1} and 0.5 mL min^{-1} for the polyamine and co-flow solvent were imaged *via* field emission scanning electronic microscopy (FESEM, Fig. 2c). The microcapsules were able to survive through the high vacuum during FESEM imaging and keep their shapes; whereas, the fractured ones collapsed immediately once cut by a razor (inset in Fig. 2c). These phenomena demonstrate that the preliminary microcapsules have walls with excellent tightness.

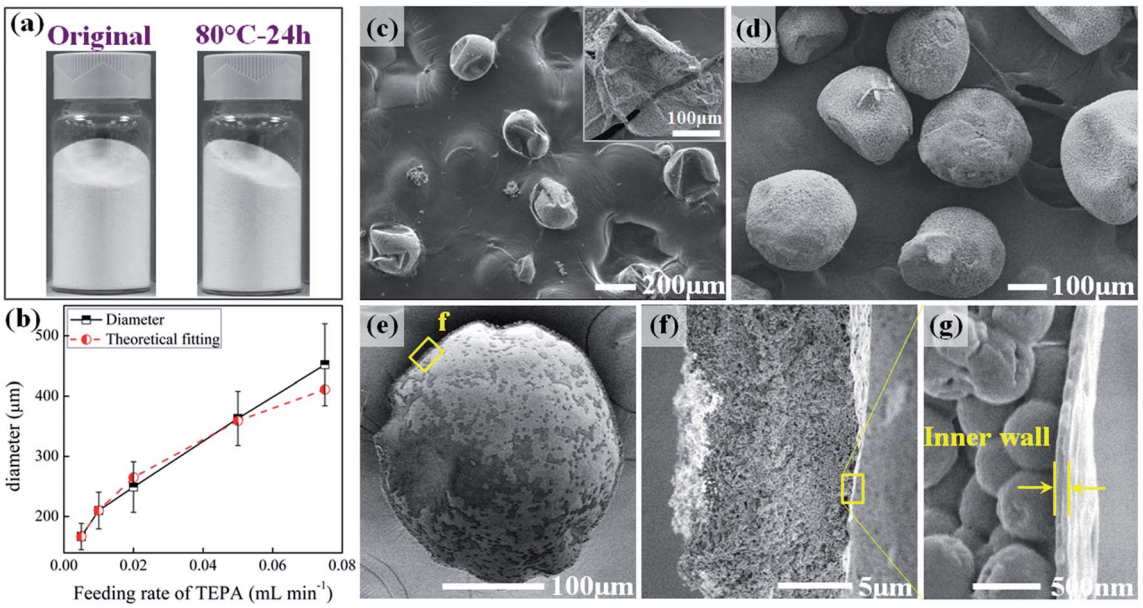

Fig. 2 (a) Appearance of fabricated TEPA microcapsules and the microcapsules after evacuation at 80 °C for 24 h. (b) Trend and theoretical fitting of microcapsule size with respect to feeding rate of TEPA when the feeding rate of co-flow solvent was fixed at 0.5 min min^{-1}. (c) Preliminary microcapsules generated right after contact of mixture from the end outlet of T2 with reaction solution. Inset shows a collapsed microcapsule after fracture. Morphology and structure of the TEPA microcapsules including (d) Overall appearance, (e) core–shell structure, (f) double-walled structure of shell, and (g) thin dense inner wall.

Notably, the location of T-junction on T2 highly influences the morphology and quality of the products. In this study, a distance of ~30 mm from the end outlet of T2 was adopted for the generation of spherical microcapsules. When it is too close, the thin continuous polyamine stream does not have enough time to break down into individual droplets before getting into the reaction solution, resulting in the formation of tube-like structures containing a liquid polyamine core rather than spherical microcapsules (Fig. S3a†). This observation offered the opportunity to *in situ* synthesize fibrous carriers containing polyamine for self-healing applications. However, when the T-junction is too far away, the interactions between the polyamine and co-flow solvent significantly influence the encapsulation process, especially when the polyamine has a relatively high solubility in the co-flow solvent. Under this circumstance, a large amount of polyurea spongy debris was generated due to the reaction between diisocyanate and the diffused/dissolved polyamine (Fig. S3b†). This debris not only caused the easy agglomeration of the microcapsules in the subsequent encapsulation process, but also decreased the quality of final microcapsules dramatically.

2.2. Properties of achieved microcapsules containing pure polyamine

Microcapsules containing pure polyamine were successfully synthesized using the proposed device and process. After collection, the microcapsules could flow free like sand without any leakage (Fig. 2a). The size of the microcapsule was tunable by varying the feeding rate of polyamine, and predictable according to the theoretical fitting based on volume transformation between the feeding rate and the reference feeding rate of 0.005 mL min^{-1} (Fig. 2b and ESI†). The morphology and structure of the pure TEPA microcapsules were characterized *via* FESEM (Fig. 2d–g). The imaged microcapsules were obtained with feeding rates of 0.02 mL min^{-1} and 0.5 mL min^{-1} for TEPA and the co-flow solvent, respectively. Due to the gradually diffused polyamine during shell formation process, shrinkage occurred for almost all the microcapsules (Fig. 2d), which is a typical feature of microcapsules synthesized *via* interfacial polymerization.[42] The cross-section of a typical microcapsule shows it has a clear core–shell structure with a big chamber inside to reserve polyamine (Fig. 2e). The shell, with a uniform thickness of ~10 μm (Fig. 2f), has a double-walled structure consisting of a thick porous outer wall and a thin dense inner wall of thickness ~100 nm (Fig. 2g). This type of structure is reasonable since the shell grows in two steps by firstly forming the preliminary polyurea membrane upon contact of the droplet with the reaction solution (Fig. 2c) and then thickening at elevated temperature. The robustness of this microcapsule originates from both the support from its thicker outer wall and the tightness of its thin but dense inner wall.

The presence of polyamine in the microcapsules was identified *via* Fourier-transform infrared (FTIR, Fig. 3a) and proton nuclear magnetic resonance (^{1}H NMR, Fig. 3b) spectroscopy. The FTIR and NMR spectra of the extracted core liquid from the TEPA microcapsules were identical to those of pure TEPA, which demonstrates the encapsulated substance is TEPA. As mentioned previously, this proposed method is not selective to the input polyamine for encapsulation. Besides pure TEPA, amine mixtures of 50TEPA50T403 (50 wt% TEPA and 50 wt% JEFFAMINE T403, similarly referred to hereinafter) and 25TEPA75T403 were also encapsulated (FESEM images in

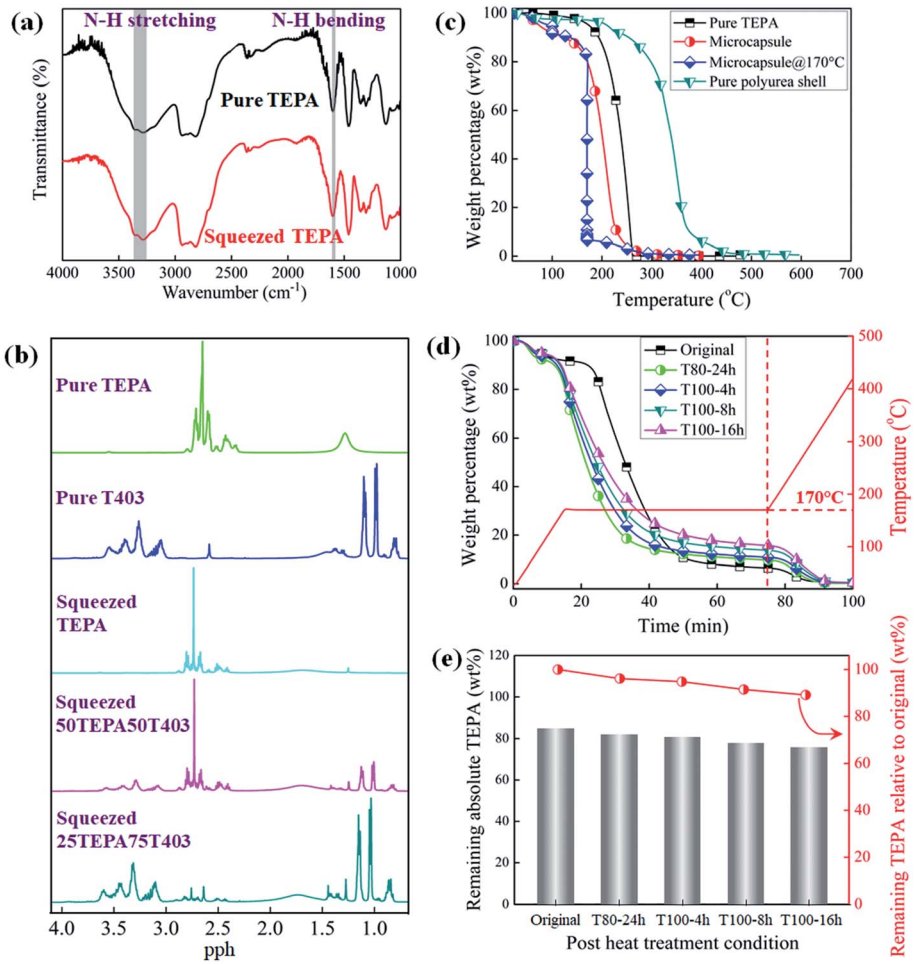

Fig. 3 (a) FTIR spectra of pure TEPA and squeezed liquid from synthesized TEPA microcapsules. (b) NMR spectra of pure TEPA, pure T403, squeezed TEPA, squeezed 50TEPA50T403, and squeezed 25TEPA75T403 from corresponding microcapsules. (c) TGA curves of pure TEPA, TEPA microcapsules, TEPA microcapsules treated isothermally at 170 °C for 60 min, and pure polyurea shell. (d) Isothermal TGA curves at 170 °C for 60 min of the original and thermally-treated TEPA microcapsules. (e) Absolute and relative weight percentage of TEPA in the original and thermally-treated microcapsules.

Fig. S4†) and characterized *via* NMR (Fig. 3b). After encapsulation, both TEPA and JEFFAMINE T403 were retained in the microcapsules. While TEPA with higher reactivity can promote healing speed, JEFFAMINE T403 with lower functionality and softer oxypropylene units can increase the fracture toughness of the healed epoxy wedge in cracks. The ease of tailoring the core composition of the microcapsules enables the convenient control of healing behavior for self-healing materials according to practical demands.

The composition and thermal stability of the microcapsules were characterized *via* thermogravimetric analysis (TGA, Fig. 3c–e). It showed that the polyurea shell is quite stable before 200 °C and its fraction in the microcapsules is only ~7 wt%, which is very low compared to microcapsules obtained *via* other processes.[28,43–46] The isothermal curve at 170 °C for 1 h for the microcapsule indicates the effective core fraction of TEPA is ~85 wt%. Due to the high thermal stability of both TEPA and the polyurea shell, these microcapsules are quite stable at temperatures up to 100 °C under high vacuum (<1 mbar). Furthermore, they could still flow freely without evident difference after thermal treatment at 80 °C for 24 h (Fig. 2a) or 100 °C for up to 16 h. The isothermal TGA curves of the thermally-treated TEPA microcapsules at 80 °C for 24 h and 100 °C for different durations are shown in Fig. 3d, and the absolute and relative remaining fraction of TEPA in the microcapsules after these thermal treatments were plotted in Fig. 3e. It shows that TEPA evaporated slowly by only ~4 wt% at 80 °C for 24 h and ~10 wt% at 100 °C for 16 h under vacuum. The final absolute TEPA in the microcapsules treated at 100 °C for 16 h was maintained above 75 wt%, which is still comparable to that of other freshly prepared microcapsules used for self-healing applications. When JEFFAMINE T403 was adopted, its thermal stability was even higher at 100 °C in contrast to that of TEPA (Fig. S5†). Polyamine microcapsules with high thermal stability are beneficial to self-healing epoxy based on it, since epoxy-based composites are commonly thermally treated at elevated temperatures during manufacturing and occasionally suffer from thermal shocks in their life cycle.

Thus, through this innovative approach, robust pure polyamine microcapsules were successfully achieved with a perfect core–shell structure, tunable and predictable size, uniform shell thickness with tight inner wall, high core content with tailorable composition, and high thermal stability. The superiority of these microcapsules for the practical application of self-healing materials was demonstrated by a self-healing epoxy with dual microcapsules containing polyamine hardener and epoxy monomer.

2.3. Quantification of performance for practical self-healing epoxy

The self-healing epoxy adopted amine microcapsules with 25TEPA75T403 and epoxy microcapsules with F10B (bisphenol F diglycidyl ether (BFDGE) diluted with 10 wt% butyl glycidyl ether (BGE)). The epoxy microcapsules were fabricated following the process established by Jin *et al.*[25] and strengthened using the coating process developed by Sun *et al.*[47] Fig. S6 and S7† show the molecular structures of BFDGE and BGE, respectively, and the synthesized epoxy microcapsules, which have good thermal stability and tightness, as verified by TGA (Fig. S8†). The healing behavior was characterized *via* the recovered mode I fracture toughness using a tapered double cantilever beam (TDCB, Fig. 4a) specimen.[48,49] This test was carried out because the quasi-static test for self-healing using TDCB is simple but well-established and comparable to other self-healing systems and fracture toughness is the most essential property for the brittle thermosetting epoxy. Both the amine microcapsules and epoxy microcapsules were dispersed uniformly in the host epoxy matrix (Fig. S9†).

This system exhibited a high healing performance due to the adopted dual microcapsules. Firstly, the influence of the ratio of amine microcapsules to epoxy microcapsules was investigated when the total concentration of the microcapsules was fixed at 10 wt% (Fig. 4b) since the stoichiometry of the released healants is crucial for any two-part self-healing system. The highest healing efficiency (η by healed peak load over original peak load, $100\% \times P_{healed}/P_{original}$) of 111 ± 12% was achieved at ratio of 1 : 1 for the dual microcapsules when the specimens were healed at room temperature (RT ~ 22–25 °C) for 48 h without any external interventions. Efficiency over 100% means full recovery, which indicates the formed epoxy wedge in cracks after healing has excellent mechanical property and good compatibility with the host epoxy matrix. Notably, a high efficiency of over 90% was obtained within a wide ratio range (2 : 3 to 2 : 1), although the released healants do not stoichiometrically match each other. This suggests the recovery is not very sensitive to the ratio of the dual microcapsules. This is important for practical application, considering the local non-uniform distribution of microcapsules and mixing issue of the released two-part healants in cracks. In contrast to the self-healing system with full recoverability using amine microcapsules containing 25TEPA75T403, the systems using microcapsules containing pure TEPA or 50TEPA50T403 showed much lower healing performances (Fig. S10†). With an increase in the concentration of JEFFAMINE T403 in the amine microcapsules, the healing efficiency increased dramatically due to the better fracture toughness of the epoxy cured by JEFFAMINE T403 compared to that by TEPA. This observation demonstrates the importance of tailoring the core composition of the adopted

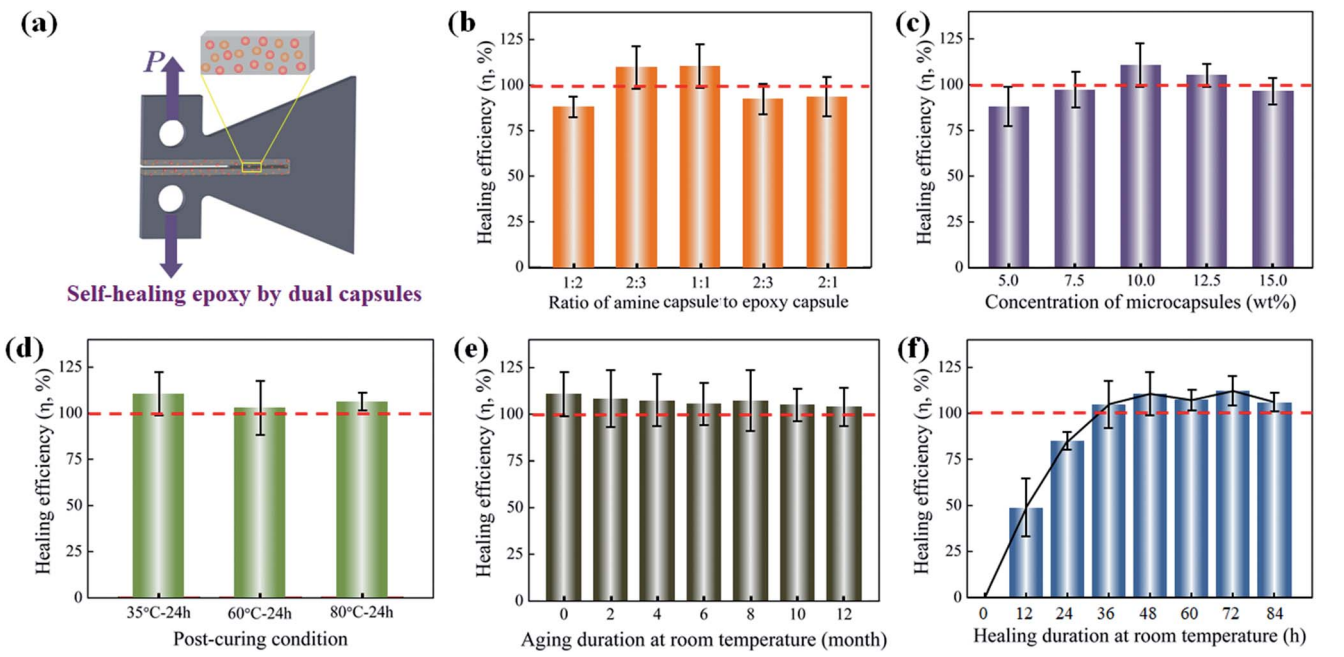

Fig. 4 Healing performance at RT in terms of recovered mode I fracture toughness. (a) Schematic TDCB specimen of self-healing epoxy by dual microcapsules using amine–epoxy chemistry. Healing efficiency regarding: (b) Ratio variation of amine microcapsules to epoxy microcapsules when total concentration is fixed at 10 wt%, (c) Total concentration of the dual microcapsules at the optimized ratio (1 : 1), (d) post-curing conditions at optimized conditions (10 wt%, 1 : 1), (e) aging duration at RT and (f) healing duration at RT at optimized conditions.

microcapsules for self-healing, which is a significant advantage of the invented encapsulation technique.

The healing performance of this self-healing epoxy regarding total concentration of microcapsules at the optimized ratio (1 : 1) is shown in Fig. 4c, with the highest efficiency at 10 wt%. Notably, a healing efficiency of ~90% (88 ± 11%) could be obtained at a concentration as low as 5 wt% and almost full recovery (97 ± 10%) could be achieved at 7.5 wt%. Since extrinsic inclusions such as microcapsules compromise some of the intrinsic mechanical properties of the host matrix,[30,50,51] high healing efficiency with less inclusions is vital for practical self-healing systems. The excellent performance of this self-healing epoxy with microcapsules at a low concentration proves the feasibility and potential of this system for practical applications.

The environmental robustness of this two-part self-healing system regarding thermal stability and long-term stability also benefits from the high quality of the microcapsules. The healing performance of the system under optimized conditions (10 wt%, 1 : 1) after thermal treatment (60 °C or 80 °C for 24 h) or RT aging for different durations was compared to that of the freshly prepared system (Fig. 4d and e, respectively). Although the healing efficiency decreased slightly, full recovery was still observed under both post-curing conditions and long-term aging up to 12 months. While this high thermal stability is attributed to the low weight loss of the encapsulated healants upon thermal treatment and insensitivity of healing to a variation in the ratio of the two healants, the outstanding long-term stability originates from the high chemical stability of the two healants isolated separately in carriers and the high tightness of the two carriers, especially the polyamine microcapsules.

The healing kinetics of this system *via* the encapsulated amine–epoxy chemistry was characterized in term of the healing efficiency with respect to healing duration at RT (Fig. 4f). Due to the high reactivity of TEPA and relatively high reactivity of JEFFAMINE T403 towards epoxy monomer, ~85% (84.9 ± 5.0%) of fracture toughness was reestablished within 24 h and full recovery (105 ± 13%) was obtained within 36 h at RT.

Finally, a fractograph of a crack at optimized condition was observed to visually examine the healing behavior (Fig. S11†). It shows the facture surfaces were perfectly wet and covered by the released healants due to the good compatibility between the cured healants and host epoxy matrix. The absence of a newly formed epoxy wedge in Fig. S11a† can be found in Fig. S11b,† which means adhesive failure, *i.e.* failure along the interface between the newly formed epoxy wedge and the fracture surface, rather than cohesive failure, *i.e.* failure in the newly formed epoxy wedge in the crack, occurred during the healing test. This failure mode suggests that the fracture toughness of the cured healants is high, attributed to the use of JEFFAMINE T403 as the encapsulated polyamine hardener. For comparison, the unhealed fracture surface with the healants rinsed away by acetone before healing and fracture surface of the specimen with only 10 wt% epoxy microcapsules were also imaged in Fig. S12.† For the former, only fractured empty microcapsules and a smooth fracture surface were observed, while for the latter, the fracture surface was only covered by a layer of epoxy liquid with the absence of polyamine hardener.

3. Conclusions

In conclusion, robust microcapsules containing pure polyamine were directly synthesized through the integration of microfluidic emulsion and interfacial polymerization, and were successfully applied in a high-performance self-healing epoxy with great potential for practical application. This integration makes full use of the advantages but avoids the shortcomings of the involved two traditional encapsulation techniques, and thus requires no stable emulsion and is not selective to the physicochemical properties of polyamines. It reconciles the aim between encapsulation and application of polyamines, and delivers microcapsules with tailorable properties according to the practical demands of self-healing materials. The fabricated dual-microcapsule self-healing epoxy shows fully autonomous recoverability with low inclusion, high thermal and long-term stability, and relatively fast healing kinetics at RT without any external interventions, which demonstrate the superiority of the achieved microcapsules and practicability of the self-healing system. Besides this practical self-healing system, the achieved polyamine microcapsules from this compounding method also enable an instant self-healing material *via* two-part amine-isocyanate chemistry and a multi-functional smart material that can fully autonomously visualize and repair damages simultaneously using the encapsulated polyamine as a multi-role trigger for both color indication and self-healing.

Conflicts of interest

There are no conflicts to declare.

Acknowledgements

We thank the SUG Grant from HKUST (R9365), the Key Program of National Natural Science Foundation of China (Grant No. 51435005), the National Instrumentation Program (Grant No. 2012YQ230043), the Science and Technology Program of Guangzhou (Grant No. 201607010240), and the Science and Technology Planning Project of Guangdong Province (Grant No. 2015B090904004, 2016A030313486, 2018A030313264), for financial support.

References

1 J. Yang, H. Zhang and M. Huang, in *Aerospace Materials Handbook*, ed. S. Zhang and D. Zhao, CRC Press, 2012, ch. 11, pp. 531–606.
2 S. R. White, N. R. Sottos, P. H. Geubelle, J. S. Moore, M. R. Kessler, S. R. Sriram, E. N. Brown and S. Viswanathan, *Nature*, 2001, **409**, 794–797.
3 D. Y. Wu, S. Meure and D. Solomon, *Prog. Polym. Sci.*, 2008, **33**, 479–522.
4 M. D. Hager, P. Greil, C. Leyens, S. van der Zwaag and U. S. Schubert, *Adv. Mater.*, 2010, **22**, 5424–5430.

5 S. R. White, B. J. Blaiszik, S. L. B. Kramer, S. C. Olugebefola, J. S. Moore and N. R. Sottos, *Am. Sci.*, 2011, **99**, 392–399.
6 J. Li, C. Nagamani and J. S. Moore, *Acc. Chem. Res.*, 2015, **48**, 2181–2190.
7 D. L. Taylor and M. I. H. Panhuis, *Adv. Mater.*, 2016, **28**, 9060–9093.
8 D. D. Chen, D. R. Wang, Y. Yang, Q. Y. Huang, S. J. Zhu and Z. J. Zheng, *Adv. Energy Mater.*, 2017, **7**, 1700890.
9 D. Y. Zhu, J. W. Guo, G. S. Cao, W. L. Qiu, M. Z. Rong and M. Q. Zhang, *J. Mater. Chem. A*, 2015, **3**, 1858–1862.
10 D. Sun, J. An, G. Wu and J. Yang, *J. Mater. Chem. A*, 2015, **3**, 4435–4444.
11 M. Scheiner, T. J. Dickens and O. Okoli, *Polymer*, 2016, **83**, 260–282.
12 I. L. Hia, E.-S. Chan, S.-P. Chai and P. Pasbakhsh, *J. Mater. Chem. A*, 2018, **6**, 8470–8478.
13 J. F. Patrick, M. J. Robb, N. R. Sottos, J. S. Moore and S. R. White, *Nature*, 2016, **540**, 363–370.
14 X. Tong, L. Du and Q. Xu, *J. Mater. Chem. A*, 2018, **6**, 3091–3099.
15 B. Zhou, D. He, J. Hu, Y. Ye, H. Peng, X. Zhou, X. Xie and Z. Xue, *J. Mater. Chem. A*, 2018, **6**, 11725–11733.
16 C. Dry, *Compos. Struct.*, 1996, **35**, 263–269.
17 D. Therriault, R. F. Shepherd, S. R. White and J. A. Lewis, *Adv. Mater.*, 2005, **17**, 395–399.
18 K. S. Toohey, N. R. Sottos, J. A. Lewis, J. S. Moore and S. R. White, *Nat. Mater.*, 2007, **6**, 581–585.
19 J. F. Patrick, K. R. Hart, B. P. Krull, C. E. Diesendruck, J. S. Moore, S. R. White and N. R. Sottos, *Adv. Mater.*, 2014, **26**, 4302–4308.
20 S. R. White, J. S. Moore, N. R. Sottos, B. P. Krull, W. A. Santa Cruz and R. C. R. Gergely, *Science*, 2014, **344**, 620–623.
21 D. Y. Zhu, M. Z. Rong and M. Q. Zhang, *Prog. Polym. Sci.*, 2015, **49–50**, 175–220.
22 M. U. Saeed, Z. F. Chen and B. B. Lin, *Composites, Part A*, 2015, **78**, 327–340.
23 R. E. Neisiany, S. N. Khorasani, J. K. Y. Lee and S. Ramakrishna, *RSC Adv.*, 2016, **6**, 70056–70063.
24 H. Jin, K. R. Hart, A. M. Coppola, R. C. Gergely, J. S. Moore, N. R. Sottos and S. R. White, Self-Healing Epoxies and Their Composites, in *Self-Healing Polymers: From Principles to Applications*, ed. W. H. Binder, 2013, ch. 15, pp. 361–376, DOI: 10.1002/9783527670185.
25 H. H. Jin, C. L. Mangun, D. S. Stradley, J. S. Moore, N. R. Sottos and S. R. White, *Polymer*, 2012, **53**, 581–587.
26 Q. Li, A. K. Mishra, N. H. Kim, T. Kuila, K.-t. Lau and J. H. Lee, *Composites, Part B*, 2013, **49**, 6–15.
27 H. Zhang and J. Yang, *J. Mater. Chem. A*, 2013, **1**, 12715–12720.
28 P. W. Chen, G. Cadisch and A. R. Studart, *Langmuir*, 2014, **30**, 2346–2350.
29 H. H. Jin, C. L. Mangun, A. S. Griffin, J. S. Moore, N. R. Sottos and S. R. White, *Adv. Mater.*, 2014, **26**, 282–287.
30 H. Zhang, P. Wang and J. Yang, *Compos. Sci. Technol.*, 2014, **94**, 23–29.
31 S. Neuser, P. W. Chen, A. R. Studart and V. Michaud, *Adv. Eng. Mater.*, 2014, **16**, 581–587.
32 D. A. McIlroy, B. J. Blaiszik, M. M. Caruso, S. R. White, J. S. Moore and N. R. Sottos, *Macromolecules*, 2010, **43**, 1855–1859.
33 J. Li, A. D. Hughes, T. H. Kalantar, I. J. Drake, C. J. Tucker and J. S. Moore, *ACS Macro Lett.*, 2014, **3**, 976–980.
34 X. Lu, J. S. Katz, A. K. Schmitt and J. S. Moore, *J. Am. Chem. Soc.*, 2018, **140**, 3619–3625.
35 H. Yi, Y. H. Deng and C. Y. Wang, *Compos. Sci. Technol.*, 2016, **133**, 51–59.
36 W. Li, C. C. Matthews, K. Yang, M. T. Odarczenko, S. R. White and N. R. Sottos, *Adv. Mater.*, 2016, **28**, 2275.
37 Y. K. Guo, L. Chen, D. G. Xu, J. R. Zhong, G. Z. Yue, D. Astruc, M. B. Shuai and P. X. Zhao, *RSC Adv.*, 2016, **6**, 65067–65071.
38 M. H. Hu, S. Peil, Y. W. Xing, D. Dohler, L. C. da Silva, W. H. Binder, M. Kappl and M. B. Bannwarth, *Mater. Horiz.*, 2018, **5**, 51–58.
39 H. Zhang, X. Zhang, Q. Chen, X. Li, P. Wang, E.-H. Yang, F. Duan, X. Gong, Z. Zhang and J. Yang, *J. Mater. Chem. A*, 2017, **5**, 22472–22479.
40 D. R. Link, S. L. Anna, D. A. Weitz and H. A. Stone, *Phys. Rev. Lett.*, 2004, **92**, 054503.
41 S. Okushima, T. Nisisako, T. Torii and T. Higuchi, *Langmuir*, 2004, **20**, 9905–9908.
42 D. Sun, H. Zhang, X.-Z. Tang and J. Yang, *Polymer*, 2016, **91**, 33–40.
43 E. N. Brown, M. R. Kessler, N. R. Sottos and S. R. White, *J. Microencapsulation*, 2003, **20**, 719–730.
44 J. L. Yang, M. W. Keller, J. S. Moore, S. R. White and N. R. Sottos, *Macromolecules*, 2008, **41**, 9650–9655.
45 M. Huang and J. Yang, *J. Mater. Chem.*, 2011, **21**, 11123–11130.
46 H. Zhang and J. Yang, *Smart Mater. Struct.*, 2014, **23**, 065003.
47 D. Sun, Y. B. Chong, K. Chen and J. Yang, *Chem. Eng. J.*, 2018, **346**, 289–297.
48 J. D. Rule, N. R. Sottos and S. R. White, *Polymer*, 2007, **48**, 3520–3529.
49 H. Jin, G. M. Miller, S. J. Pety, A. S. Griffin, D. S. Stradley, D. Roach, N. R. Sottos and S. R. White, *Int. J. Adhes. Adhes.*, 2013, **44**, 157–165.
50 Y. C. Yuan, M. Z. Rong, M. Q. Zhang, B. Chen, G. C. Yang and X. M. Li, *Macromolecules*, 2008, **41**, 5197–5202.
51 H. Zhang and J. Yang, *Smart Mater. Struct.*, 2014, **23**, 065004.